

Supplementary Information

New water soluble nickel(II) and copper(II) oxime complexes containing acid group: DNA interaction investigations

Murat Biltekin, Cansu Gökçe Topkaya* & Ramazan Güp

Department of Chemistry, Faculty of Science, Mugla Sıtkı Koçman University, Mugla, Turkey

E-mail: cansutopkaya@mu.edu.tr

Received 10 November 2023; accepted (revised) 23 February 2024

DNA binding studies

The complex's DNA binding ability was examined using UV-Vis and fluorescence spectroscopy, with minor alterations to the previously published literature.³¹⁻³⁴ At room temperature, titrations were carried out with a buffer containing 10 mM Tris-HCl and 50 mM NaCl (pH 7.6). The complicated stock solution was made using 1% (V/V) DMF and 99% (V/V) Tris-HCl buffer. CT-DNA (lyophilized) was dissolved in Tris-HCl buffer overnight at 4 °C and utilized within 2 days as a DNA stock solution. A solution of CT-DNA gave a ratio of UV absorbance at 260 and 280 nm of ca. 1.8–1.9:1, indicating that the DNA was sufficiently free of protein. The DNA concentration was determined from the absorbance at 260 nm using the molar absorption coefficient ($6600 \text{ M}^{-1} \text{ cm}^{-1}$) at 260 nm.

UV-Visible absorption studies

By adding increasing quantities of CT-DNA (0-100 M) to a constant concentration of complex (25 M), absorption titrations were performed. The reaction mixture was allowed to incubate for 5 minutes before the absorption spectrum was recorded. After each addition, the intrinsic binding constant K_b of complex was calculated by using Wolfe-Shimmer equation (Eq. 1).³⁷

$$[\text{DNA}]/(\epsilon_a - \epsilon_f) = [\text{DNA}]/(\epsilon_b - \epsilon_f) + 1/K_b(\epsilon_b - \epsilon_f) \quad (\text{Eq. 1})$$

where $[\text{DNA}]$ is the concentration of DNA in base pairs, ϵ_a , ϵ_f , and ϵ_b correspond to $A_{\text{obs}/[\text{compound}]}$, the extinction coefficient for the free complex, and the extinction coefficient for the complex fully bound with DNA. In plot of $[\text{DNA}] / (\epsilon_a - \epsilon_f)$ versus $[\text{DNA}]$, the intrinsic binding constant K_b is given by the ratio of the slope to y-intercept.

Viscosity measurements

Viscosity experiments were carried out using an Ubbelodhe viscometer at room temperature. The viscosity of CT-DNA solution (25 μM) was measured in the absence and presence of increasing amounts of the compound (6.25-50 μM) in tris-HCl buffer (10 mM tris-HCl-NaCl; pH=7.6) containing %5 DMF solution. Flow time was measured three times with a digital stopwatch. Viscosity values were presented as $(\eta/\eta_0)^{1/3}$ versus concentrations of [complex]/[DNA] where η was the viscosity value for DNA in presence of the compounds and η_0 was the viscosity value of CT-DNA alone.

DNA cleavage studies

Plasmid DNA (pBR322) cleavage study of the complex was performed by agarose gel electrophoresis. Stock solution of complex was prepared in DMF and diluted with Tris-HCl buffer to desired concentrations. Supercoiled (SC) DNA (pBR322) (25 ng/ μL , 5 μL) in Tris-HCl (100 mM, pH 7.6) was treated with 100 μM of the complex in a total volume of 30 μL , and then incubated at 37 $^\circ\text{C}$ for 1-6 h with 1 h intervals in the presence and absence of H_2O_2 (5 mM) to obtain the optimal cleavage incubation time. The optimal complex concentrations for cleavage were also studied using the same methodology but with different complex concentrations (25, 50, 75, 100 and 250 M). After incubation, the reaction was quenched with 4 liters of loading buffer (0.25 percent bromophenol blue, 30 percent glycerol, 0.25 percent xylene cyanol, and 10 mM EDTA) and loaded on a 1 percent agarose gel with 1 g/mL ethidium bromide. In TBE buffer (40 mM Tris/borate and 1 mM EDTA, pH 8.0), electrophoresis was performed at 80 V for 1.5 hours. UV light was used to photograph and visualize the bands. ROS inhibitors [DMSO (200 M, hydroxyl radical scavenger), KI (150 M, superoxide radical scavenger), and NaN_3 (150 M, singlet oxygen scavenger)], catalase (15 U, hydrogen peroxide scavenger), and groove binders [DAPI (200 M, minor groove binder) and MG (200 M, major groove binder)] were used to investigate the mechanism. Prior to the addition of complex, these agents were introduced to pBR322 DNA. Further analysis was carried out as previously stated.

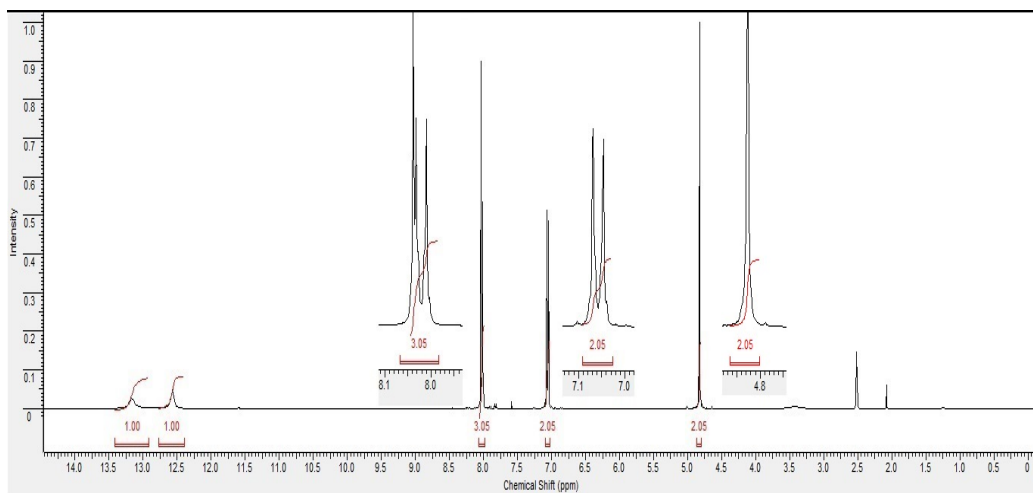


Figure S1: ^1H NMR spectrum of compound H_2L^1

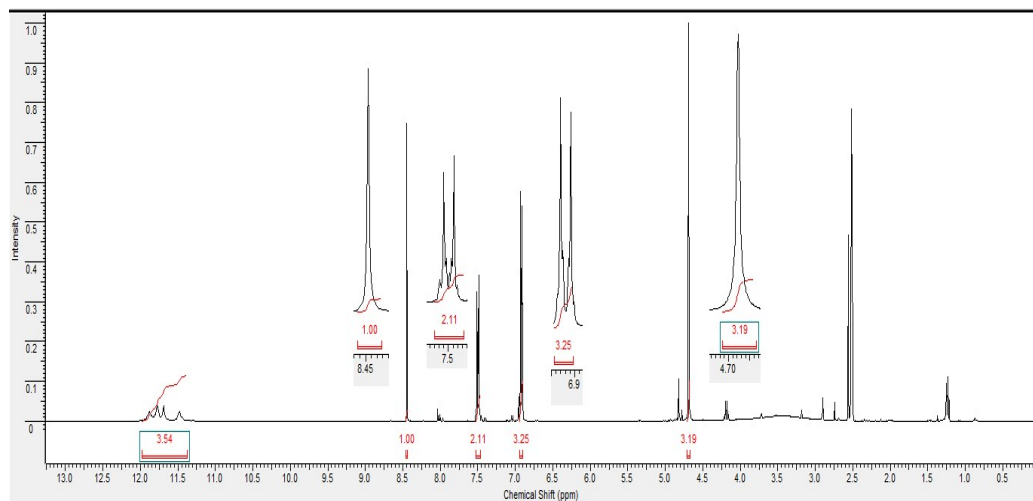


Figure S2: ^1H NMR spectrum of compound H_3L^2

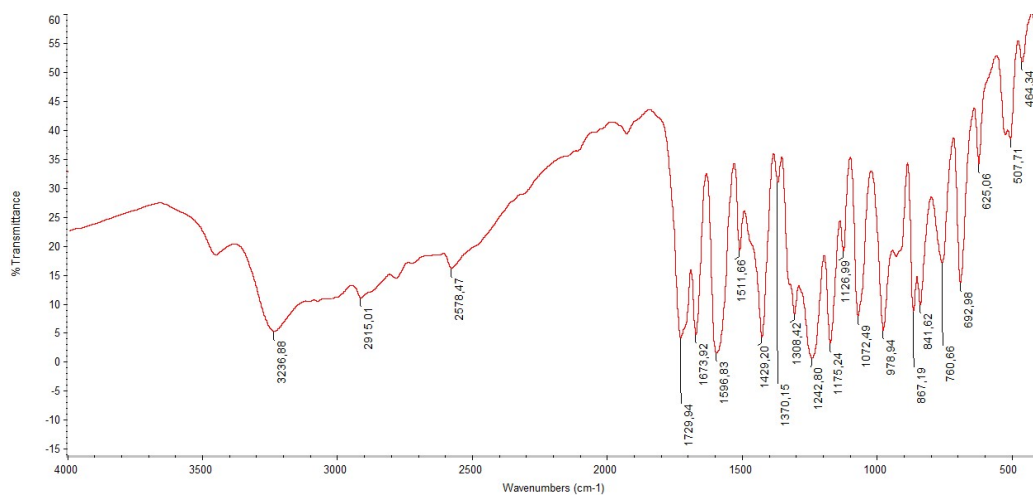


Figure S3: FTIR spectrum of compound H₂L¹

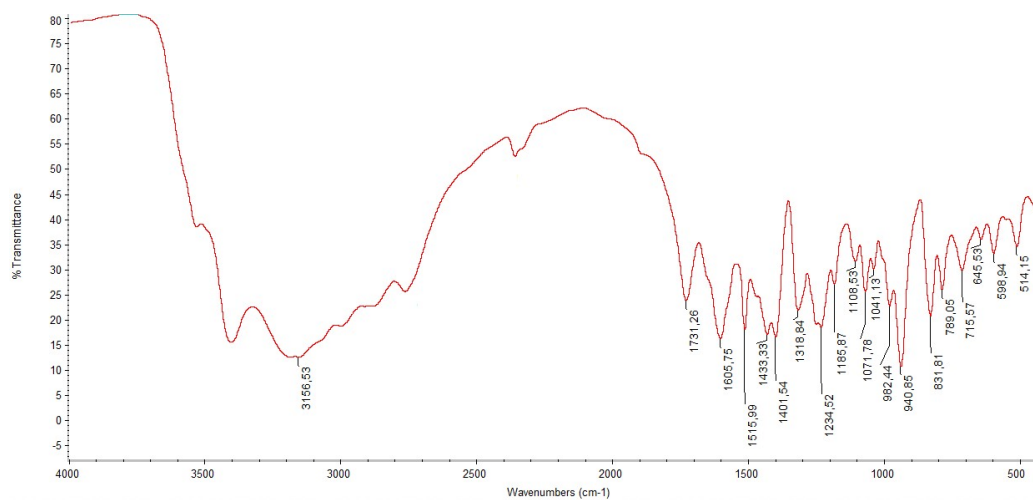


Figure S4: FTIR spectrum of compound H₃L²

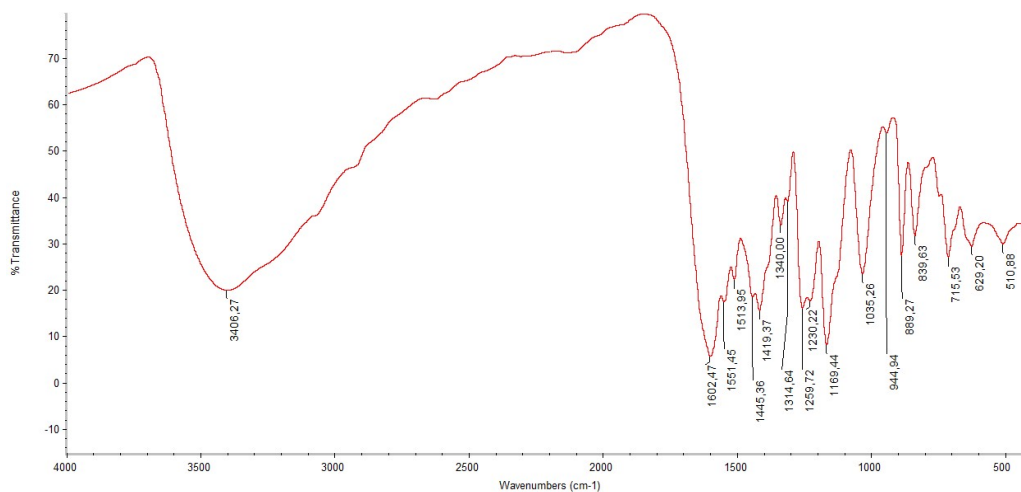


Figure S5: FTIR spectrum of compound $[\text{Cu}_n(\text{L}^1)_n(\text{CH}_3\text{COO})_n] \cdot 2\text{H}_2\text{O}$

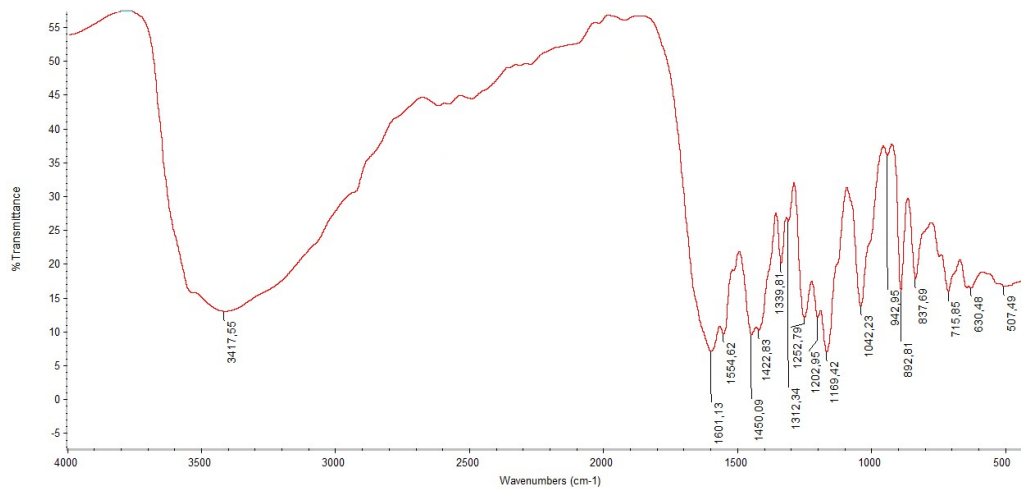


Figure S6: FTIR spectrum of compound $[\text{Ni}_n(\text{L}^1)_n(\text{CH}_3\text{COO})_n] \cdot 2\text{H}_2\text{O}$

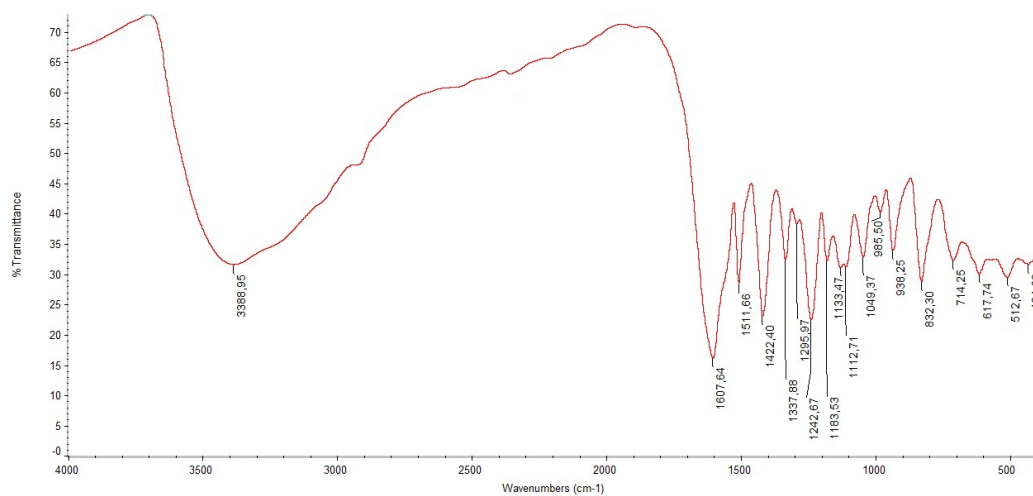


Figure S7: FTIR spectrum of compound $[\text{Cu}_2(\text{L}^2)(\text{H}_2\text{O})_2] \cdot 4\text{H}_2\text{O}$

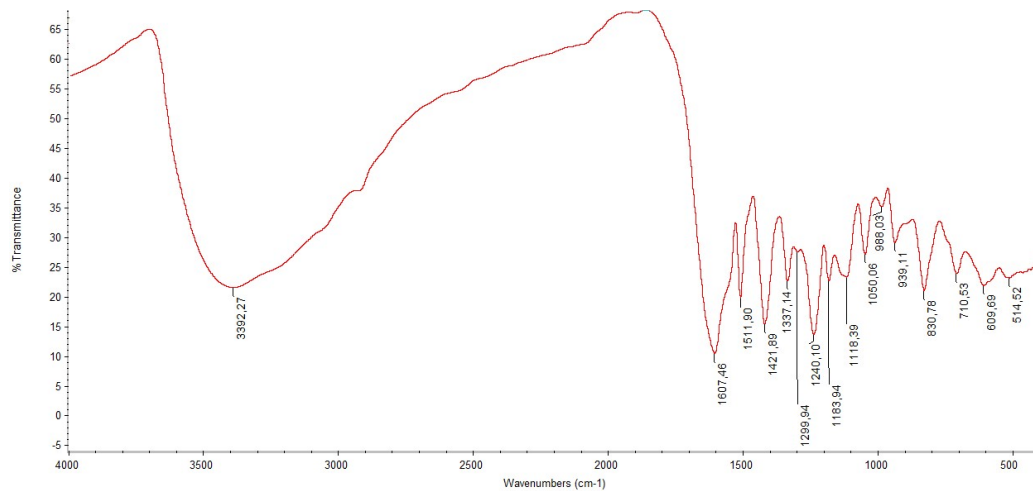


Figure S8: FTIR spectrum of compound $[\text{Cu}_2(\text{L}^2)(\text{H}_2\text{O})_2] \cdot 2\text{H}_2\text{O}$

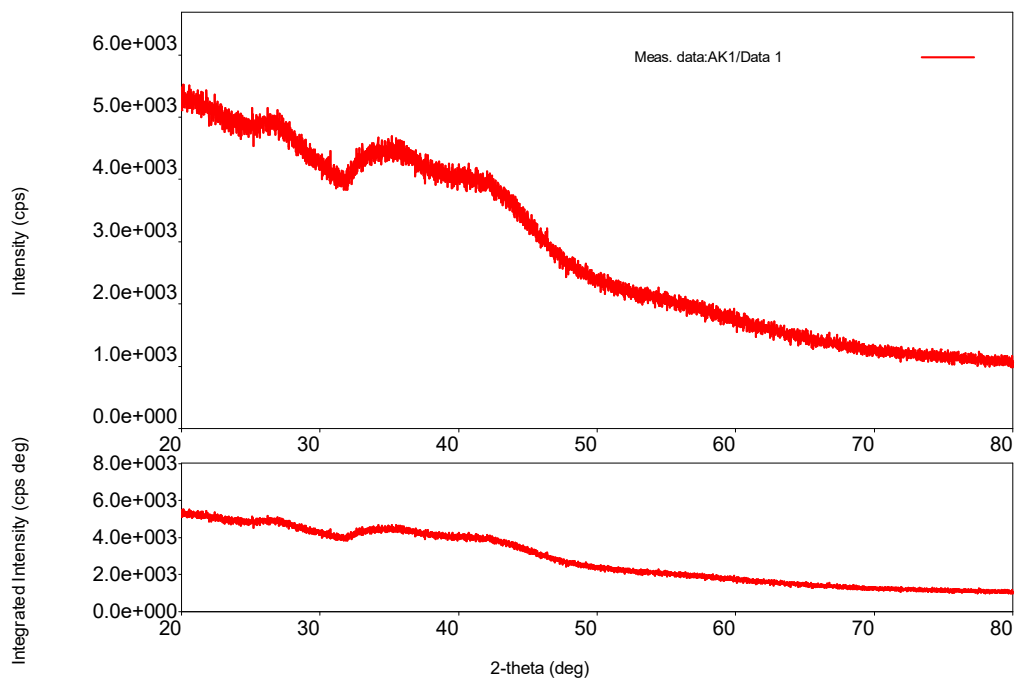


Figure S9: XRD spectrum of compound $[\text{Cu}_n(\text{L}^1)_n(\text{CH}_3\text{COO})_n] \cdot 2\text{H}_2\text{O}$

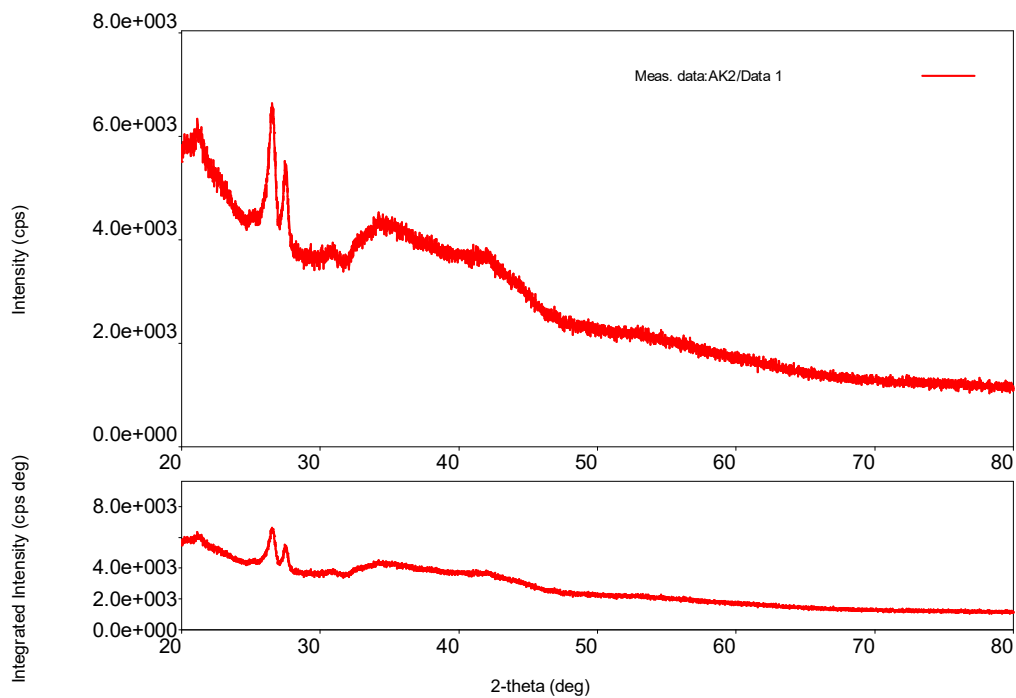


Figure S10: XRD spectrum of compound $[\text{Ni}_n(\text{L}^1)_n(\text{CH}_3\text{COO})_n] \cdot 2\text{H}_2\text{O}$

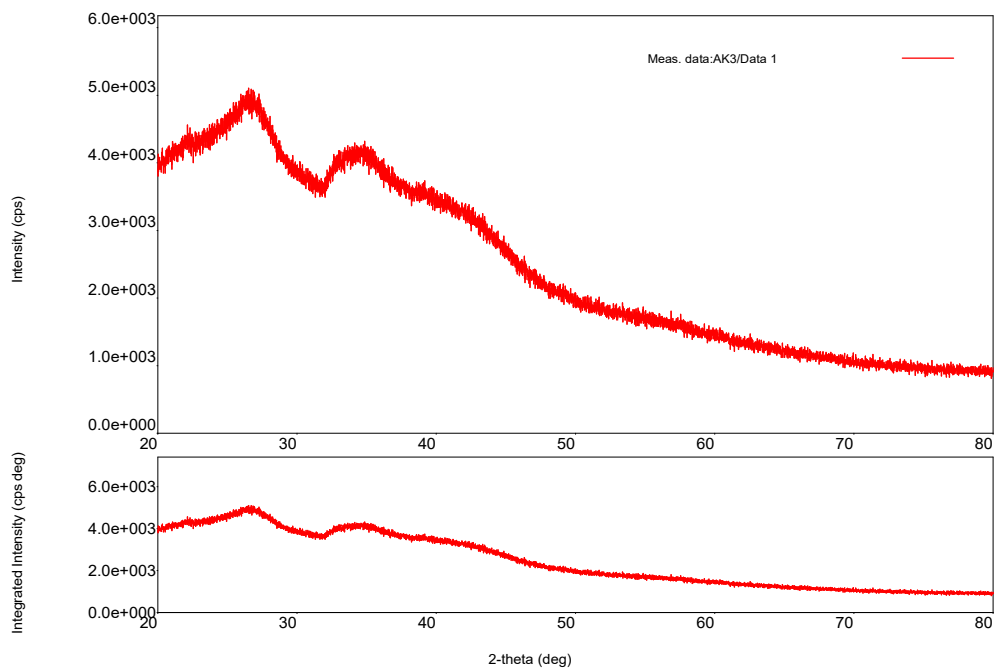


Figure S11: XRD spectrum of compound $[\text{Cu}_2(\text{L}^2)_2(\text{H}_2\text{O})_2]\cdot 4\text{H}_2\text{O}$

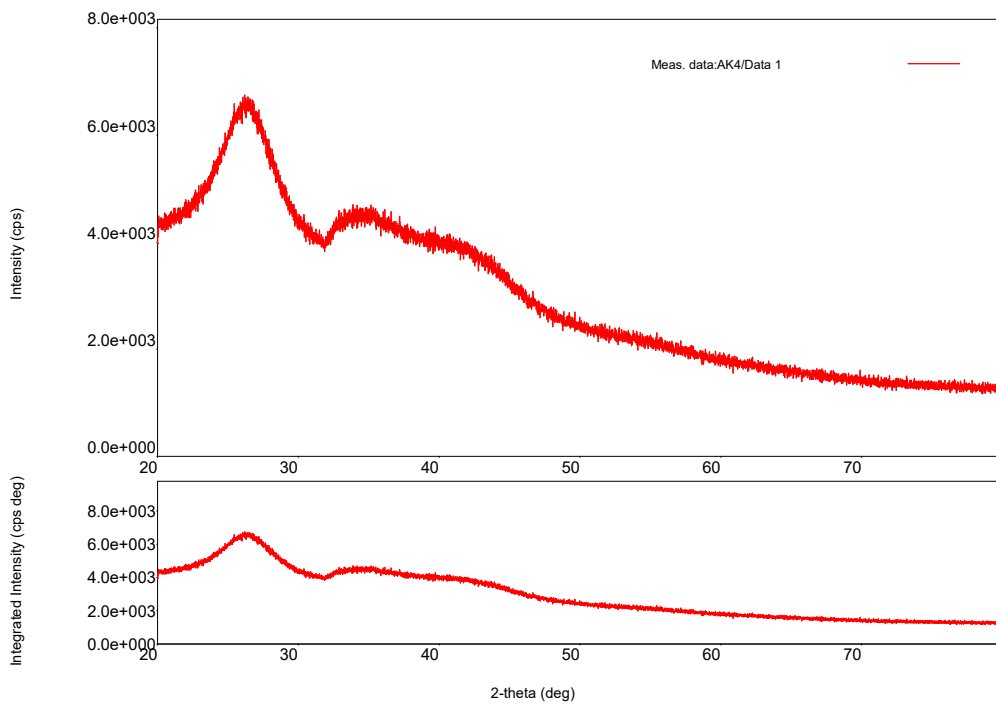


Figure S12: XRD spectrum of compound $[\text{Ni}_2(\text{L}^2)_2(\text{H}_2\text{O})_4]\cdot 2\text{H}_2\text{O}$

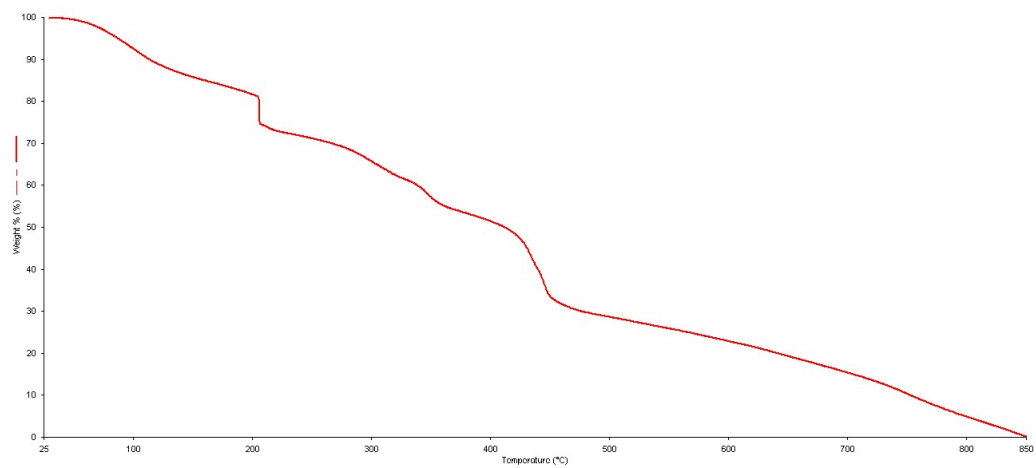


Figure S13: TGA spectrum of compound $[\text{Cu}_n(\text{L}^1)_n(\text{CH}_3\text{COO})_n] \cdot 2\text{H}_2\text{O}$

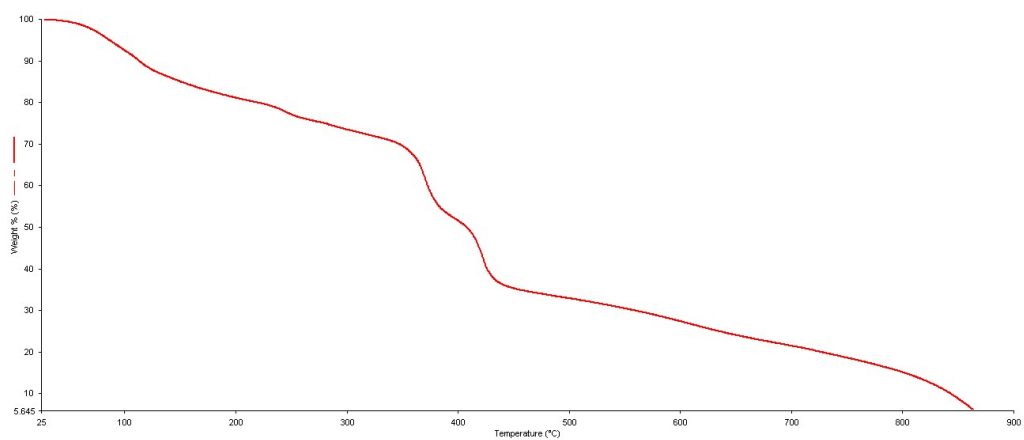


Figure S14: TGA spectrum of compound $[\text{Ni}_n(\text{L}^1)_n(\text{CH}_3\text{COO})_n] \cdot 2\text{H}_2\text{O}$

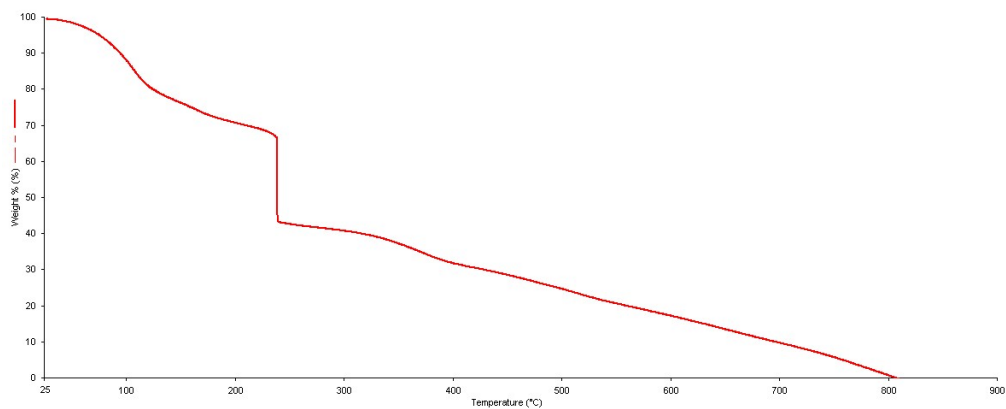


Figure S15: TGA spectrum of compound $[\text{Cu}_2(\text{L}^2)_2(\text{H}_2\text{O})_2] \cdot 4\text{H}_2\text{O}$

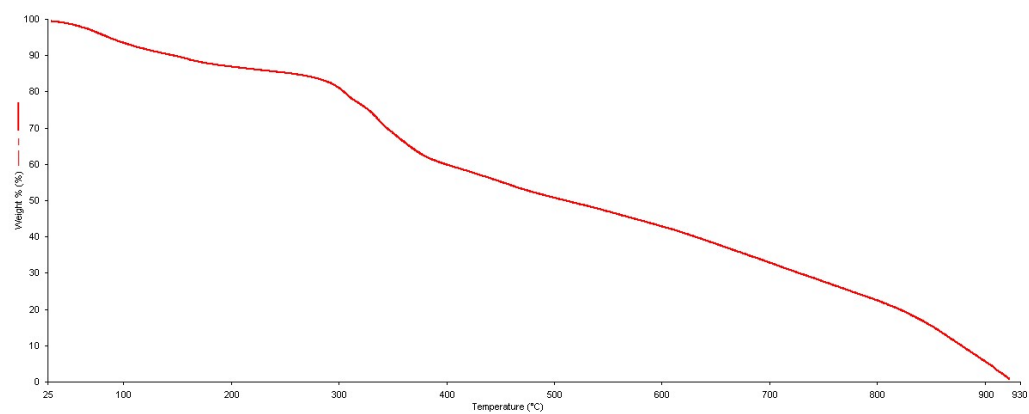


Figure S16: TGA spectrum of compound $[\text{Ni}_2(\text{L}^2)_2(\text{H}_2\text{O})_4] \cdot 2\text{H}_2\text{O}$

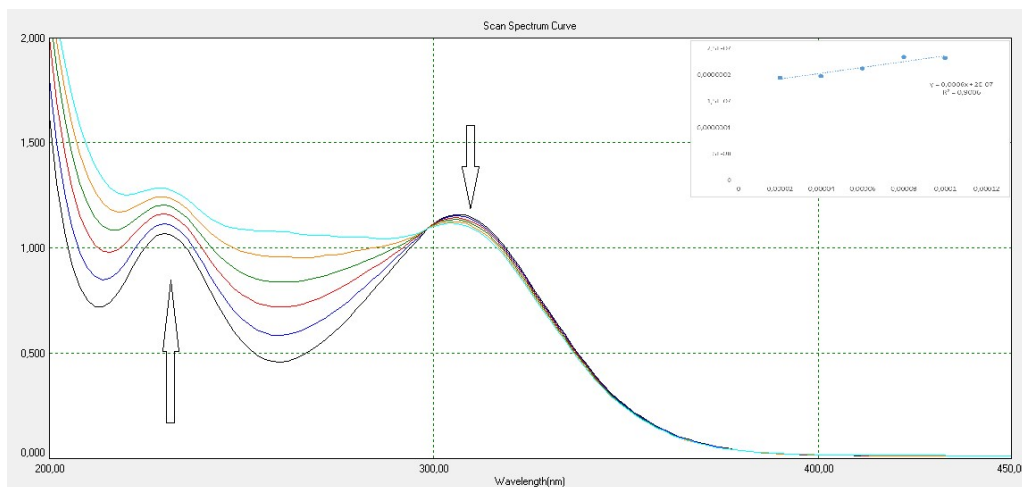


Figure S17: CT-DNA binding spectrum of compound H_2L^1

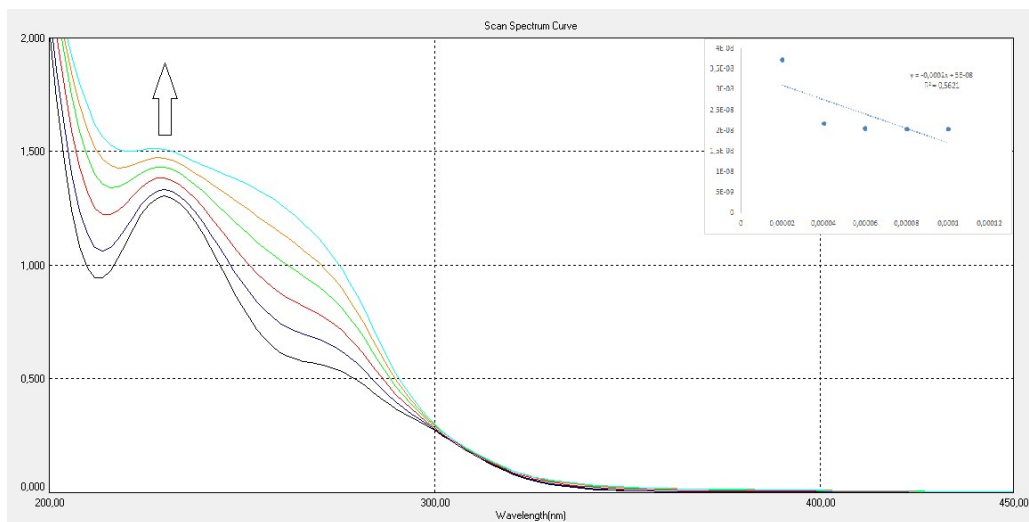


Figure S18: CT-DNA binding spectrum of compound H_3L^2

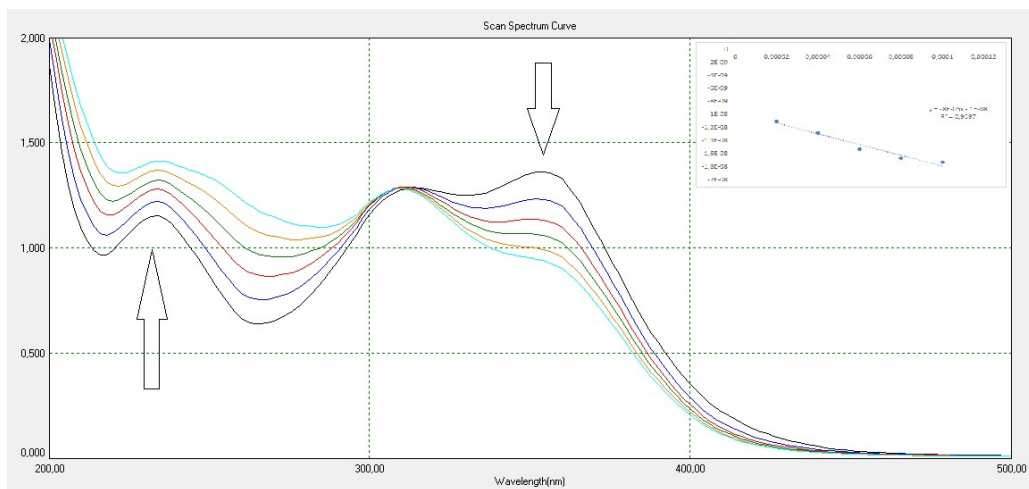


Figure S19: CT-DNA binding spectrum of compound $[Cu_n(L^1)_n(CH_3COO)_n] \cdot 2H_2O$

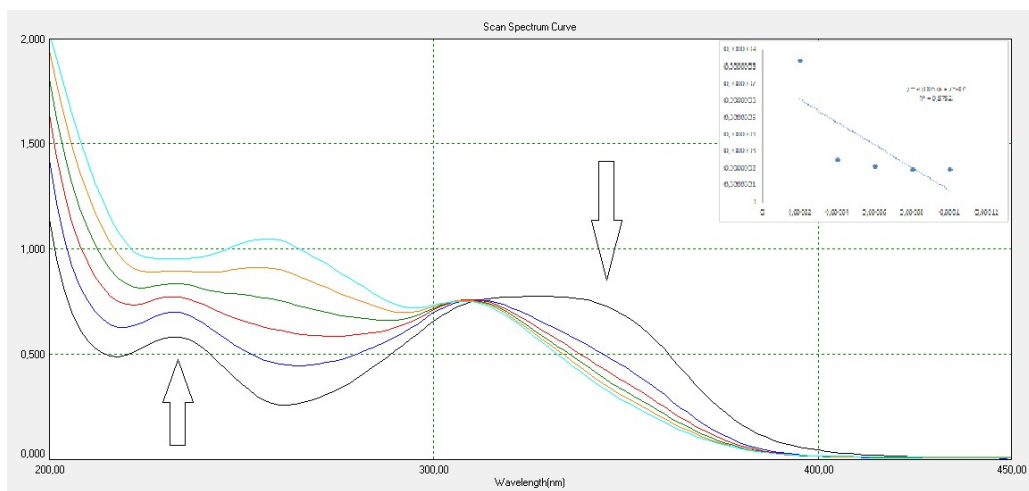


Figure S20: CT-DNA binding spectrum of compound $[\text{Ni}_n(\text{L}^1)_n(\text{CH}_3\text{COO})_n] \cdot 2\text{H}_2\text{O}$

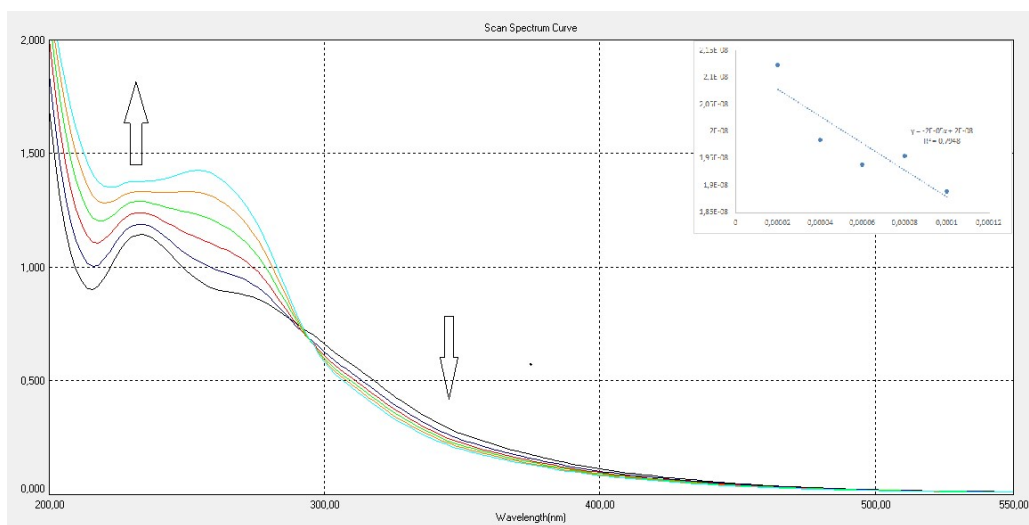


Figure S21: CT-DNA binding spectrum of compound $[\text{Cu}_2(\text{L}^2)_2(\text{H}_2\text{O})_2] \cdot 4\text{H}_2\text{O}$

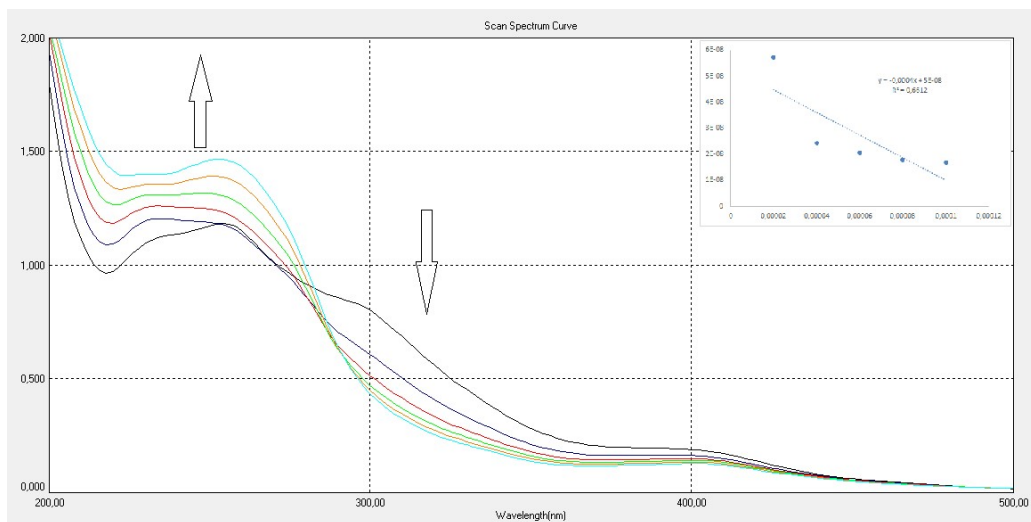


Figure S22: CT-DNA binding spectrum of compound $[\text{Ni}_2(\text{L}^2)_2(\text{H}_2\text{O})_2] \cdot 2\text{H}_2\text{O}$